DEPARTMENT OF THEORETICAL PHYSICS AND COMPUTER MODELLING

Head of Department *Dr. hab. phys*. Eugene Kotomin

Research Area and Main Problems

Our theoretical research interests are focused on six classes of problems related to:

- kinetics of diffusion-controlled processes, with emphasis on pattern formation and catalytic surface reactions;
- the atomic and electronic structure of numerous advanced materials, with emphasis on calculations of properties of defects, surfaces, metal/insulator interfaces.
- theoretical simulations and experimental studies of nanostructures and nanomaterials;
- modeling of advanced functional materials for energy applications (fuel cells, ceramic membranes, Li batteries, fusion and fission reactors);
- gyrotron development for thermonuclear reactors

We combine several different techniques, including analytical formalisms and large-scale computer simulations (quantum chemical methods, stochastic simulations as well as Monte Carlo/cellular automata modeling) as described in our homepage http://www1.cfi.lu.lv/teor

Staff

Laboratory of kinetics in self-organizin.g systems	Laboratory of computer modeling of electronic structure of solids
Dr. O. Dumbrajs (full member of Latvian Acad. Sci.)	Dr. D. Bocharov
Dr. D. Gryaznov	Dr. R. Eglitis (corr. member of Latvian Acad.Sci.)
Dr. E. Klotins	Dr. Yu. Mastrikov
Dr. hab. E. Kotomin (full member of Latvian Acad. Sci.)	Dr. S. Piskunov
Dr. hab. V. Kuzovkov	Dr. hab. Yu. Shunin
Dr. A. Popov	Dr. Yu. Zhukovskii
Dr. G. Zvejnieks	B.S. A. Chesnokov
M.S. J. Shirmane	M.S. A. Gopejenko
B.S. Moskina	B.S. J. Kazerovskis
	B.S. O. Lisovski
	M.S. A. Platonenko
	M. Sokolov

Scientific visits abroad

1. Dr. hab. E. Kotomin, Max-Planck Institut für Festkörperforschung, Stuttgart, Germany (8 months), Eurasian National University, Astana, Kazakhstan (2 weeks), Photochemistry Center, Russian Academy of Sciences, Moscow, Russia (10 days)
2. Dr. O. Dumbrajs, Fukui University, Japan (3 months)
3. Dr. A. Popov, Laue-Langevin Institute, Grenoble, France (1 week); Institute of Materials Science, Darmstadt University of Technology, Germany (1 week); Institute of Physics, University of Tartu (2 weeks), CIEMAT, Spain (1 week)
4. Dr. D. Bocharov, University of Duisburg-Essen, Germany (1 month)
5. Dr. Yu. Mastrikov, Institute of Applied Materials, Karlsruhe, Germany (3 weeks), Eurasian National University, Astana, Kazakhstan (2 weeks)
6. Dr. S. Piskunov, University of Duisburg-Essen, Germany (6 weeks), Laboratori Nationali di Frascati, Italy (1 month); Institute of General and Inorganic Chemistry, Russia, Moscow (2 months)
7. Dr. hab. Yu. Shunin, Laboratori Nationali di Frascati, Italy (1 month); Institute of General and Inorganic Chemistry, Moscow, Russia (1 week)
8. Dr. Yu. Zhukovskii, St. Petersburg State University, Russia (3 weeks), Institute of General and Inorganic Chemistry, Moscow, Russia (2 weeks)
9. B.S. A. Chesnokov, University of Duisburg-Essen, Germany (2 weeks)
10. B.S. J. Kazerovskis, University of Ulm, Germany (10 months)
11. B.S. O. Lisovski, Uppsala University, Sweden (10 months)

International Cooperation

Belarus	1. Institute of Nuclear Problems, Belarusian State University, Minsk (Prof. S. A. Maksimenko)
China	2. Beijing Institute of Technology, Beijing (Dr. H. Shi).
Estonia	3. Institute of Physics, University of Tartu (Prof. A. Lushchik)
Finland	4. Helsinki University of Technology, Espoo (Dr. T. Kurki-Suonio)
France	5. Laue-Langevin Institute, Grenoble, Prof. H. Schober)
Germany	6. Max Planck Institut für Festkörperforschung, Stuttgart (Prof. Dr. J. Maier) 7. Deutsches Elektronen-Synchrotron DESY, Hamburg (Dr. A. Kotlov) 8. Darmstadt University of Technology, Darmstadt (Prof. H von Seggern) 9. Institut für Hochleistungsimpuls & Mikrowellentechnik (KIT), Karlsruhe (Dr. S. Kern, Dr. B. Piosczyk) 10. Institut für Angewandte Materialien (KIT), Karlsruhe (Dr. A. Möslang, Dr. P. Vladimirov) 11. Dept of Theoretical Chemistry, Univ. Duisburg-Essen (Prof. E. Spohr)
Israel	12. Ben Gurion University, Beer Sheva (Prof. D. Fuks)
Italy	13. Laboratori Nazionali di Frascati (Dr. S. Bellucci, Dr. M. Cestelli-Guidi)
Kazakhstan	14. Gumilyov Eurasian National University, Astana (Prof. A.T. Akilbekov)
Japan	15. FIR Center, University of Fukui (Prof. T. Idehara)
Lithuania	16. Institute of Semiconductor Physics (SPI), Vilnius (Dr. E. Tornau)

Poland	17. Warsaw University, Department of Chemistry (Prof. A. Huczko, Prof. A. Dąbrowska) 18. Institute of Physics, Academy of Science, Warsaw (Prof. H. Szymczak)
Romania	19. University of Craiova (Dr. D. Constantinescu)
Russia	20. St. Petersburg State University, Petrodvorets (St. Petersburg) (Prof. R.A. Evarestov) 21. Institute of General and Inorganic Chemistry, Russian Academy of Sciences, Moscow (Prof. P.N. Dyachkov) 22. Photochemistry Center, Russian Academy of Sciences, Moscow (Prof. A.A. Bagaturyants)
Spain	23. Centro de Investigaciones Energeticas Medioambientales y Tecnologicas (CIEMAT), Madrid (Dr. R. Vila)
UK	24. University College London (Prof. A.L. Shluger)
Ukraine	25. Ivan Franko National University, Lviv (Prof. O. I. Aksimentyeva, Prof. I. Bolesta, Dr. I. Karbovnyk)
USA	26. University of Maryland, College Park (Dr. G.S. Nusinovich, Dr. M.M. Kukla)

Main Results

A. Electronic structure calculations for advanced materials

HYBRID HARTREE-FOCK-DENSITY FUNCTIONAL THEORY CALCULATIONS OF OXYGEN VACANCY TRANSPORT IN COMPLEX PEROVSKITE OXIDES

D. Gryaznov, E.A. Kotomin

S. Baumann,

Forschungszentrum Jülich, Institute for Energy Research, IEF-1, Mater. Synth . Processing, Jülich, Germany

R. Merkle

Max Planck Institute for Solid State Research, Stuttgart, Germany

The hybrid HF-DFT calculations based on the PBE0 functional and the LCAO basis set were combined with the permeation measurements, in order to analyze the formation enthalpy of oxygen vacancies $V_O^{\bullet\bullet}$ in complex perovskite solid solutions, like (La,Sr)$FeO_{3-\delta}$ (LSF) with different Sr doping. The use of hybrid functionals allowed us to reproduce the bulk properties of these solid solutions and their behavior as semiconductors.

The correctness of band gap is important to calculate the formation enthalpy of $V_O^{\bullet\bullet}$ in LSF which is in agreement with previous experimental

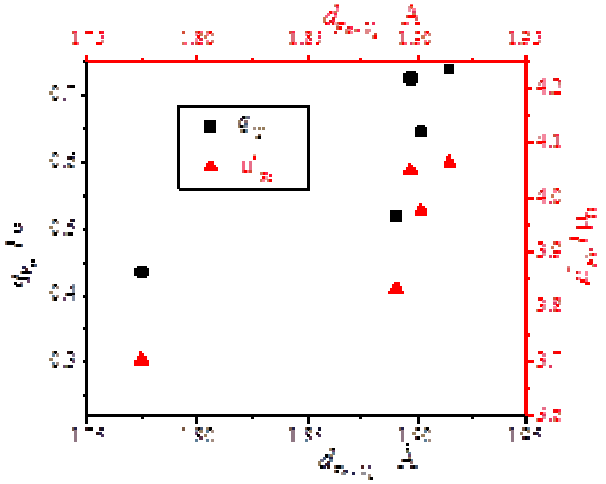

Figure 1. The Mulliken charge of $V_O^{\bullet\bullet}$ and magnetic moment on Fe depending on $d_{Fe-V_O^{\bullet\bullet}}$ for LSF with 12.5% doping (40 atom supercell with the nonstoichiometry δ = 0.125).

studies on the formation enthalpy of $V_O^{\bullet\bullet}$ in LSF. Moreover, the LCAO basis set allowed us to determine the electronic charge density within the vacancy (due to additional so-called ghost basis set at the vacancy site) and find the correlation between the charge of $V_O^{\bullet\bullet}$, the Fe-$V_O^{\bullet\bullet}$ distance and the magnetic moment on Fe. It is demonstrated that a careful comparison of the calculation results with the experiments requires the knowledge on the oxidation state of Fe under experimental conditions and thus the relation between nonstoichiometry δ and Sr doping.

We have confirmed that the formation enthalpy of $V_O^{\bullet\bullet}$ significantly decreases with the Sr doping which greatly accelerates oxygen transport through permeation membranes and SOFC cathodes and thus improves their performance.

AB INITIO THERMODYNAMICS OF OXYGEN VACANCIES AND ZINC INTERSTITIALS IN ZnO

E.A. Kotomin,
T.S. Bjørheim
Centre for Materials Science and Nanotechnology, Department of Chemistry, University of Oslo, Norway

ZnO is an important wide band gap semiconductor with potential application in various optoelectronic devices. Recently, we have explored the thermodynamics of oxygen vacancies and zinc interstitials in ZnO based on first principles phonon calculations. While formation enthalpies are evaluated using hybrid DFT calculations, phonons are addressed using the PBE and the PBE+*U* functionals. The phonon contribution to the formation entropy of oxygen vacancies is similar for all functionals, while that of zinc interstitials is significantly lower with PBE+*U* than PBE (Fig. 2), and we suggest that the former functional is more suited for investigating vibrational properties of ZnO.

Further, the phonon contribution to the entropy is most dominant for oxygen vacancies, and their Gibbs formation energy increases when including phonons. Hence, phonons decrease the formation energy difference of oxygen vacancies and zinc interstitials and render their equilibrium concentrations more comparable at the very highest temperatures. The analysis of the phonon density of states (Fig.3) shows additional band due to oxygen vacancies which could be used for defect detection.

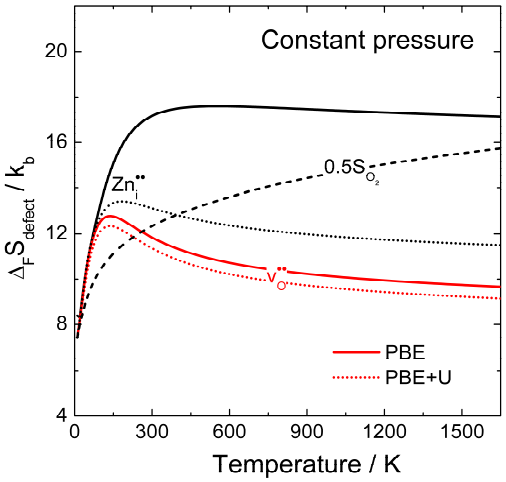

Figure 2. Defect formation entropy from PBE and PBE+*U* of $Zn_i^{\bullet\bullet}$ and $V_O^{\bullet\bullet}$.

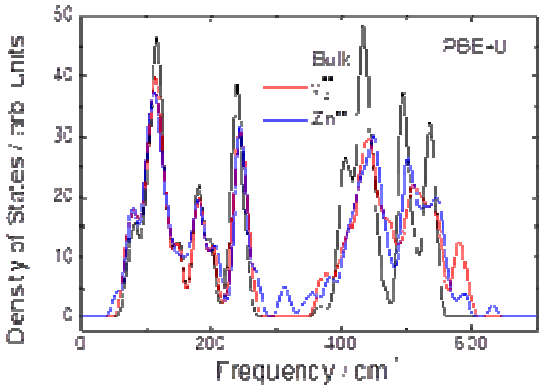

Figure 3. Phonon density of state of pure ZnO, and cells with $V_O^{\bullet\bullet}$ and $Zn_i^{\bullet\bullet}$ defects, calculated at the Γ-point of the 3×3×2 supercell.

HYDROGEN-INDUCED METALLIZATION OF ZnO($1\bar{1}00$) SURFACE: FIRST PRINCIPLES STUDY

E.A. Kotomin, J. Purans, Yu.F. Zhukovskii
A. Usseinov, A.T. Akilbekov
Gumilyov Eurasian National University, Astana, Kazakhstan

To improve ZnO thin film production technologies, the effect of hydrogen on the structural and electronic properties of different zinc oxide surfaces have been studied. Specifically, during the growth of ZnO crystalline samples, the highest growth rates were achieved along the *z*-axis and most favorable facets were found to be ($1\bar{1}00$) and ($11\bar{2}0$) characterized by comparatively low surface energies. Meanwhile, the former has been found by us as slighly more stable. Large scale *ab initio* calculations on H/ZnO($1\bar{1}00$) system have been performed combining the basis set of linear combination of atomic orbitals (LCAO) method with the hybrid exchange-correlation Perdew–Burke–Ernzerhof (PBE0) functional as has been implemented in the *CRYSTAL2009* computer code. For simulation of hydrogen adsorption on the ($1\bar{1}00$) surface, the slab model of finite thickness along the *z* axis and extended by (2×2) in the *x* and *y* directions corresponding to the periodic distribution of hydrogen adatoms has been chosen.

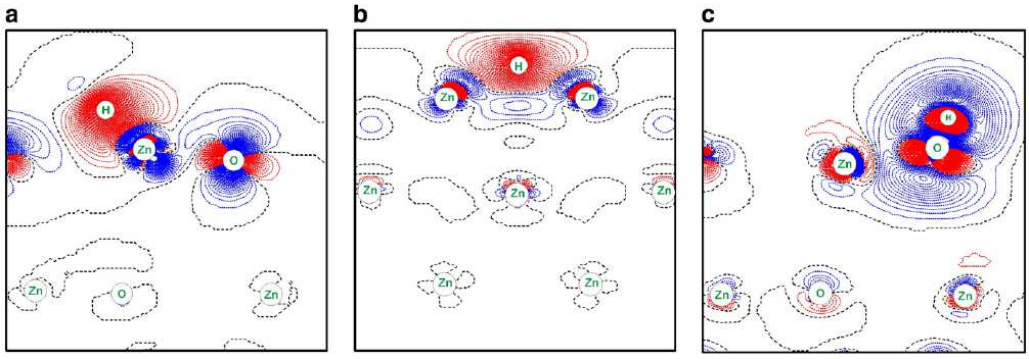

Figure 4. Differential electron density plots are drawn for the hydrogen atom upon the ZnO($1\bar{1}00$) surface positioned a) atop surface Zn ion; b) atop surface O ion; and c) atop the hollow position. The solid (red) and dotted (blue) isolines correspond to positive (excess) and negative (deficiency) electron density, respectively. Increment for isolines is 0.001 *e* within the range from −0.1 to 0.1 *e*.

We have studied adsorption of hydrogen atoms over different surface sites (Fig. 4) varying their concentration *per* unit cell. Energetically the most preferable adsorption sites have been found adatom positions atop the surface oxygen ion. Hydrogen adatoms also reduce the surface energy of ZnO($1\bar{1}00$) making it more stable (0.35 *vs.* 0.73 J/m^2) Since hydrogen atoms are mainly produced by dissociation of H_2 molecules, the adsorption energy with such the reference state are smaller by half of its binding energy (*i.e.*, 1.58 eV). Electron densiy distrbutions for H adatoms atop suface Zn (Fig. 4a), hollow (Fig. 4b) and O (Fig. 4c) sites clearly confirm results of total nergy calculations. O-H bond population on the substrate is much larger than that in the bulk (0.215 *vs.* 0.137 *e*). Electron charge redistribution cleary shows strong bonding around O sites and anti-bonding in the proximity of surface Zn ions. A comparison with ionic displacements on a perfect surface shows that both surface O and Zn ions are displaced outwards and preserve the same ordering: O ions lie higher than Zn ions. The density of states for adatom in three different positions clearly show that even at 25% coverage the adsorbed hydrogen shows the density of states in the energy range overlapping the bottom of conduction band, thus transforming ZnO thin films into a conducting state (metallization). An increase of hydrogen coverage up to 1 ML leads to a disappearance of the band gap at all.

AB INITIO MODELING OF RADIATION DAMAGE IN MgF_2 CRYSTALS

E.A. Kotomin, S. Piskunov,

F.U. Abuova, A.T. Akilbekov,

Gumilyov Eurasian National University, Astana, Kazakhstan

V.M. Lisitsyn,

Tomsk Polytechnical University, Tomsk 634003, Russia

MgF_2 with a rutile structure is important radiation-resistant material with numerous applications due to its transparency from vacuum ultraviolet to infrared range of photon energies. Optical devices (e.g., lenses and windows) produced from magnesium fluoride are transparent over an extremely wide range of photon energies, from vacuum ultraviolet to infrared. Another advantage of MgF_2 is high radiation stability: concentrations of stable radiation defects therein are 3–5 orders of magnitude smaller than in alkali halide crystals. Theoretical study has been based on the large scale *ab initio* DFT-LCAO calculations using hybrid B3PW exchange–correlation functional and atomic basis set.

The primary radiation defects are Frenkel pairs of fluorine vacancies with trapped electrons (*F* centers) and interstitial fluorine atoms which rapidly form the diatomic F_2^- molecules (called the *H* centers) with a regular F^- ion (Fig. 5). The formation energy of the close Frenkel pair has been found to be 8.36 eV. The distance between the *F* and *H* centers is 1.85 Å only. An interatomic distance within *H* center (diatomic molecule) is 1.87 Å, considerably less than in free *H* center (1.96 Å).

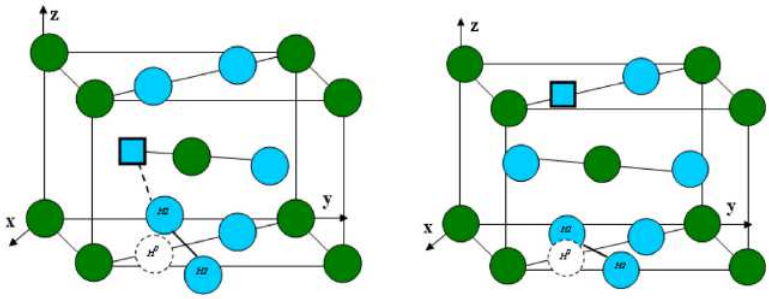

Figure 5. The nearest (left) and well separated (right) *F*–*H* (110) pairs in MgF_2. Blue (light) atoms are fluorine ions, green (dark) magnesium ions. Dotted circle indicates position of a regular fluorite ion before the *H* center formation. The *F* center is marked as a square while the *H* center consists of the *H*1 and *H*2 ions.

The electronic density plot for a close *F*–*H* pair (Fig. 6) confirms a strong anisotropy of the charges in the hole center and their strong mutual perturbation. Only ions nearest to the pair are slightly perturbed.

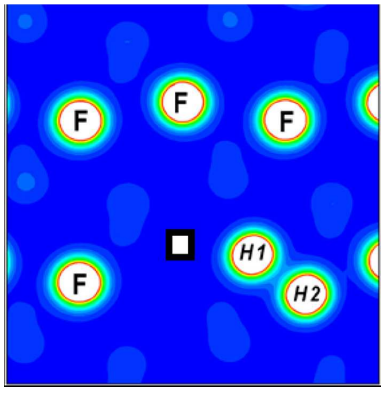

Figure 6. The total electronic charge distribution for the nearest *F*–*H* pair. Red colored lines correspond to 0.40 *e* while density inside dark blue area lies within interval 0.000-0.002 *e* (other details are described in Fig. 5).

AB INITIO CALCULATIONS OF SURFACE AND DEFECTS FOR ABO_3 PEROVSKITE OXIDES AND MeF_2 FLUORITES

R.I. Eglitis

We have summarized recently in the review the results of calculations on surface relaxations, energetics, and bonding properties for ABO_3 perovskite (001), (011) and (111)

surfaces using mostly a hybrid description of exchange and correlation is presented. Both AO and BO_2-terminations of the nonpolar (001) surface and A, BO, and O terminations of the polar (011) surface, as well as B and AO_3-terminations of the polar (111) surface were considered. Upon the AO-terminated (001) surface, all upper-layer A atoms relax inward, while second layer atoms relax outwards. For the BO_2-terminated (001) surface, in most cases, the largest relaxations are on the second-layer metal atoms.

For almost all ABO_3 perovskites, the surface rumpling is much larger for the AO-terminated than for the BO_2-terminated (001) surface, but their surface energies always are quite similar. In contrast, different terminations of the (011) ABO_3 surface lead to very different surface energies for the O-terminated, A-terminated, and BO-terminated (011) surface, respectively. A considerable increase in the Ti-O or Zr-O, respectively, chemical bond covalency near the (011) surface as compared both to the bulk and to the (001) surface in ABO_3 perovskites were predicted. According to the results of ab initio calculations for Nb doped $SrTiO_3$, Nb is a shallow donor; six nearest O ions are slightly displaced outwards from the Nb ion.

The *F* center in ABO_3 perovskites resembles the electron defects in the partially-covalent SiO_2 crystal rather than usual F centers in ionic crystals like MgO and alkali halides. The results of calculations for several perovskite $KNb_xTa_{1-x}O_3$ (KTN) solid solutions, as well as hole and electron polarons in ABO_3 perovskites are analyzed.

The *H* center, a hole trapped at an interstitial anion site, placed in the bulk and at the (111) surface of calcium fluoride CaF_2, has been studied by using DFT with B3PW hybrid exchange potentials. The *H* center is oriented in the (111) direction in the bulk case and along the (100) direction in the surface case (Fig. 7), and the hole is mainly localized on the interstitial fluorine. The surface *H* center leads to a remarkable XY-translation of the surface atoms. The hole induces an empty energy levels in the β-spin in the band gap, located 2.9 eV above the valence band (VB) top, corresponding to the first optical absorption band, and the surface effect heightens the hole level considerably.

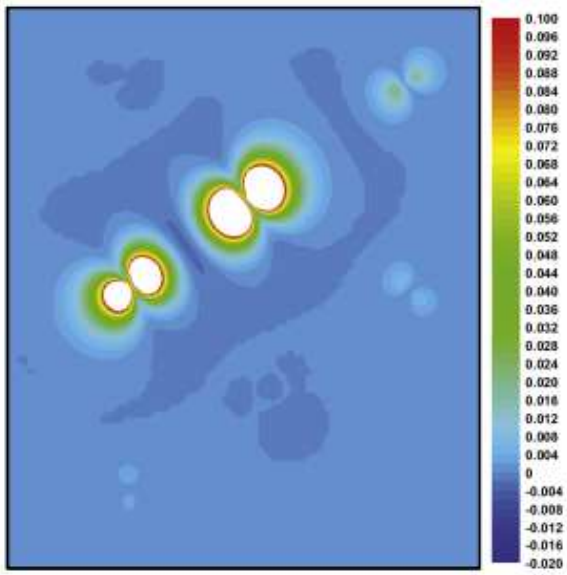

Figure 7. Electron spin density contours in CaF_2 with the *H* center in configuration *H*(111) from the (110) side view (details are explained in Figs. 5,6).

Density of states (DOS) calculations reveal that the hole band mainly consists of the *H*-center *p*-orbitals (Fig. 7), and the interstitial fluorine does the major contribution. Further study regarding the electron-hole pair, named *F-H* pair, in this paper, shows that the geometrical structure is similar to an *F* center and an *H* center paired together, whereas the hole localized on the *H* center in the isolated *H*-center case, moves to the fluorine vacancy (V_F) site. The electron-hole pair induces seven defect levels in the VB-CB gap, three of them located near the Fermi energy, being occupied, and four of them located above the Fermi level, forming the hole bands. The *p*-orbitals of the interstitial fluorine form the three electron bands and the four hole bands are composed of the *s*- and *p*-orbitals of the V_F.

RADIATION DEFECTS IN COMPLEX PEROVSKITE SOLID SOLUTIONS

E.A. Kotomin, Yu.A. Mastrikov,

M.M. Kuklja,
Materials Science and Engineering Dept., University of Maryland, College Park, USA

J. Maier
Max Planck Institute for Solid State Research, Stuttgart, Germany

Recently, we have presented and discussed the results of first principles calculations of (Ba,Sr)(Co,Fe)O_3 known as BSCF perovskite solid solutions (Fig. 8a) containing basic point defects (cation and anion vacancies, cation exchange, and antisite defects), as well as structural and Schottky disorders have quite low formation energies and are energetically favorable. The calculated cation exchange energies are very low on both the *A*- and *B*- sublattices (Ba↔Sr and Co↔Fe) of the cubic perovskite structure; this should lead to an easy aggregation of cations with further phase separation. In contrast, antisite defects (*A*↔*B* exchange) are costly and unlikely to contribute to disorder in these materials. The oxygen interstitials form so-called dumbbell (split) configuration with a regular oxygen ions (Fig.8b). Thus, in general, complex perovskite solid solutions (for example, double perovskites) can accommodate much more expressed defect disorder than parent ABO_3 perovskites. An analysis of possible BSCF decomposition into different phases or binary oxides was also performed.

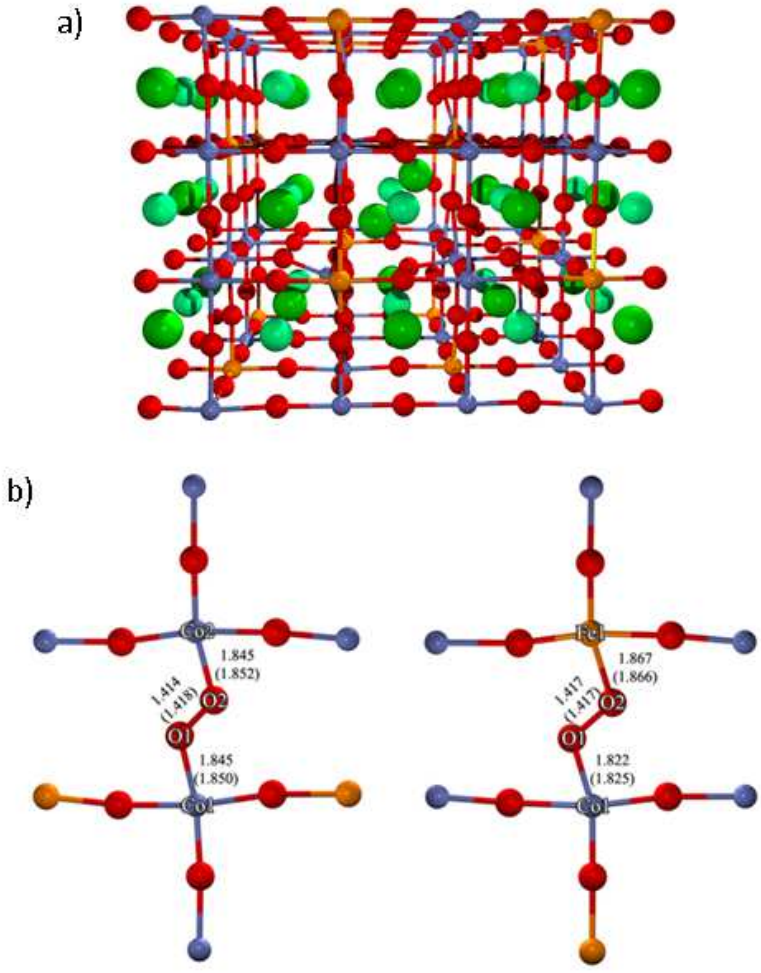

Figure 8. (a) Ba-split interstitial configuration is shown in the 320 atom model supercell of BSCF, (b) and (c) two different configurations of O split interstitial defects. The numbers indicate distances between atoms in a close Frenkel pair.

AB INITIO SIMULATIONS OF POINT DEFECTS (VACANCIES) AND ATOM SUBSTITUTES (O AND Y) IN *fcc*-Fe LATTICE

A. Gopejenko, Yu.F. Zhukovskii, E.A. Kotomin

A. Möslang, P. Vladimirov
Institut für Angewandte Materialien, Karslsruhe Institut für Technologie (KIT), Karlsruhe, Germany

V.A. Borodin
State Research Center "Kurchatov Institute", Moscow, Russia

Current generation of reduced activation ferritic-martensitic steels (RAFM) strengthened by oxides permits a growth of the operating temperature for future fusion and advanced fission reactors by 100°C (up to 650°C and higher). The most frequently used oxide for the strengthening of RAFM steels is Y_2O_3, as it is one of the most stable oxides with melting temperature higher than that of the steels which might play significant role in the formation of oxide nanoparticles in oxide disperse-strengthened (ODS) steels.

The main goal of this study is to get deep insight in the formation of the ODS particles inside RAFM steel structures. To perform it, a two-step theoretical approach for atomistic simulation of this process is proposed. The *first step* includes extensive *ab initio* calculations of elementary yttrium and oxygen complexes inside the iron lattice (4×4×4 and 5×5×5 *fcc*-Fe supercell models) containing also Fe-vacancies (V_{Fe}) performed using VASP computer code. Both interaction energies between solute and matrix atoms and barriers for migration of different solute atoms are extracted from these calculations for further atomistic simulations.

Binding energies between the impurity atoms and vacancies as well as their migration barrier energies are important parameters for the LKMC modeling of the ODS particle formation (the *second step* of simulations). To perform calculations for estimating migration barriers, the nudge elastic band (NEB) method have been used (as implemented in the *VASP* computer code). The lowest calculated energy of the barrier for Y atom migration has been found to be about 1.75eV. Obviously, the increased concentration of V_{Fe} vacancies is required for interstitial Y migration and the increased size of the supercell is necessary for this aim.

AB INITIO AND ELECTROMAGNETIC SIMULATIONS OF CNT GROWTH UPON Fe-Pt NANOCLUSTERS

Yu.N. Shunin, Yu.F. Zhukovskii, S. Piskunov,

V.I. Gopeyenko, N.Yu. Burlutskaya, T.D. Lobanova—Shunina,
Information Systems Management Institute, Riga, Latvia

S. Bellucci, F. Micciula
INFN-Laboratori Nazionali di Frascati, Frascati, Italy

Carbon nanotubes (CNTs) of various chiralities open new wide possibilities for modern nanoelectronics as promising candidates for nanointerconnects in a high-speed electronic nanosensoring and nanomemory devices. We focus our current study on the implementation of advanced simulation models for a proper description of the fundamental electromagnetic properties (electrical resistance, capacitances and impedances) in contacts between carbon nanotubes of different morphologies and metallic substrates of different nature. We also present the model of magnetically stimulated CNT growth for a special case of Fe-Pt metallic

nanoclusters (Fig. 9), which have unique magnetic properties. We have performed optimization of nanocluster shape (icosahedral or cuboctahedral), morphology (onion-like or striped) and equilibrium ratio between Fe and Pt atoms (for this aim, we have performed first principles DFT-LCAO calculations). It has been found that the energetically most preferable configuration of nanocluster is onion-type $Fe_{43}Pt_{104}$ icosahedron with external Pt shell (Fig. 9). We expect that in the presence of magnetic field, the CNTs growth will be more determined from the point of view of possible nanotube morphologies. Moreover, the creation of a CNT forest based on Pt-Fe nanoparticles (Fig. 10) provides the possibilities to consider this kind of structure as the basic fragment of nanomemory devices, where information bits are located in nanoparticles and the CNT forest provides the necessary spin transport for reading and recording information. The parametrically controlled production of carbon nanotubes (CNTs) with predefined morphologies is a topical technological problem for modern nanoelectronics. This process can be streamlined using even minor diamagnetic properties of carbon atoms at the expense of magnetic field and strong induced ferromagnetism of the nanoparticle.

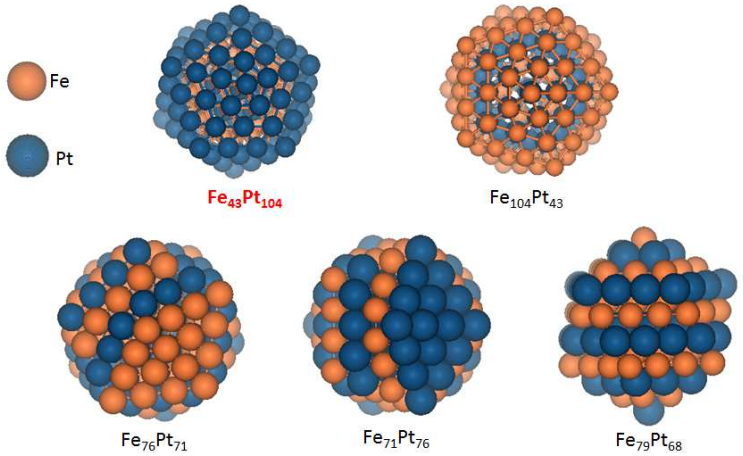

Figure 9. Equilibrium configurations of Fe-Pt nanoclusters with morphologies of onion-type (top level) and striped icosahedra.

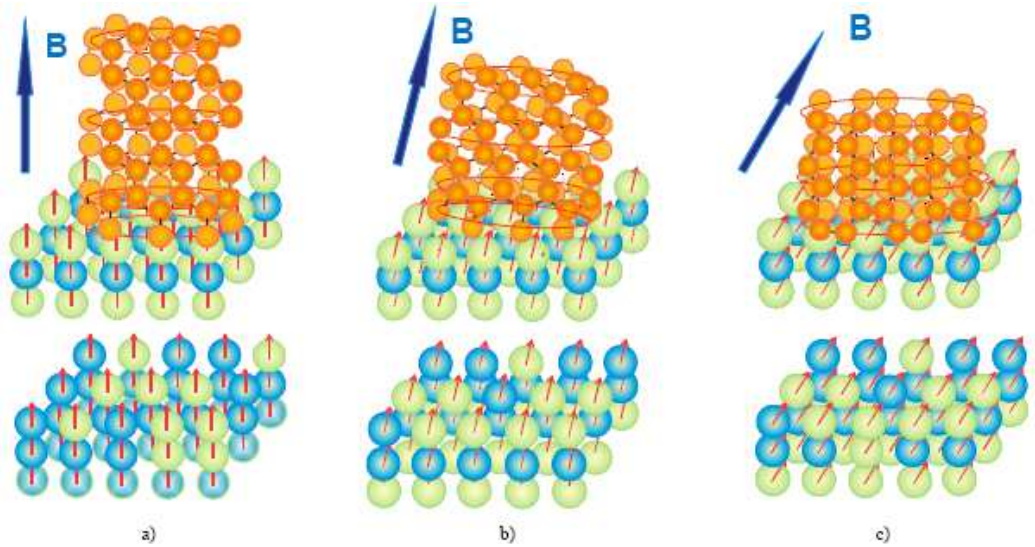

Figure 10. Magnetically stimulated orientation of magnetic moments of atoms in model interconnects during the CNTs controlled growth with the expected chiralities under the directed magnetic field with the orientation angle shown by arrows, where **B** is the magnetic induction and the chirality angle is $\phi = \Theta_B$: a) arm-chair CNT, $\phi = 0$; b) chiral CNT, $0 < \phi < 30^o$; c) zig-zag CNT, $\phi = 30^o$.

The morphology of Fe-Pt cluster and its atomic structure (including the short-range order) play a primary role in the process of CNT growth stimulated by the magnetic field. Nucleation in the process of CNT growth in cases of the ordered Fe-Pt nanoclusters hase been found to be more stable and has principal advantages relatively to the controlled CNT growth as compared to the cases of any kinds of anisotropic Fe-Pt nanocatalysts.

B. Kinetics of processes with self-organization

STATIC AND DYNAMIC SCREENING EFFECTS IN ELECTROSTATIC SELF-ASSEMBLY OF NANO-PARTICLES

V.N. Kuzovkov and E.A. Kotomin

Kinetics of processes in nanomaterials, e.g. nanoparticles in soft matter or liquid phase is of great importance for many applications. In the description of charge screening in electrostatic self-assembly of nanoparticles (molecules) embedded into a polar solvent, the *static* screening effects (a contribution associated with the rapid spatial redistribution of small and highly mobile ions of a solvent) is traditionally treated phenomenologically, using the Yukawa short-range potential for describing the interaction between these particles. However, this model has a limited range of applicability being valid only for infinitely diluted systems and high salt concentrations. During a slow self-assembling process with nanoparticle formation, very dense structural elements (aggregates) are formed, in which the distances between the nanoparticles could become comparable to the Debye radius in the Yukawa potential. For such the structural elements *dynamic* screening effects (the contribution of nanoparticles themselves into the screening potential) becomes important.

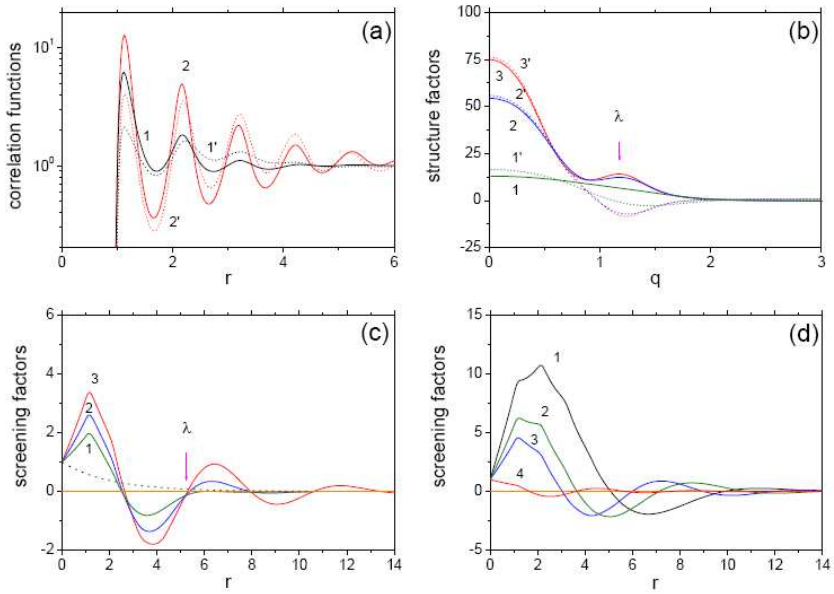

Figure 11. Ionic binary systems with Lennard-Jones and Coulomb interactions (weak static screening). (a) Joint correlation functions; (b) Structure factors; (c) Screening factors for the same times as in window (b); (d) Sreening factors at fixed time and for different values of Bjerum length.

Using a novel integrated approach (nonlinear integro-differential kinetic equations for the correlation functions of particles, Fig. 11), we have obtained the self-consistent solution in 3d case and compare roles of both static (equilibrium) and dynamic (nonequilibrium) charge screening effects in different situations. This is a continuation of our recent study)], with the polar solvent effects now taken into account.

STATISTICAL CHARACTERIZATION OF SELF-ASSEMBLED CHARGED NANOPARTICLE STRUCTURES

G. Zvejnieks, V.N. Kuzovkov and E.A. Kotomin

We proposed a novel approach for description of dynamics of nano-structure formation for a system consisting of oppositely charged particles. The combination of numerical solution of analytical Bogoliubov-Born-Green-Kirkwood-Yvon (BBGKY) type equation set with reverse Monte Carlo (RMC) method allows us to overcome difficulties of standard approaches, such as kinetic Monte Carlo or Molecular Dynamics, to describe effects of long range Coulomb interactions. Moreover, this allows one to study the system dynamics on realistic time and length scales.

We applied this method to a simple short-range Lenard-Jones (LJ)-like 3d system and 2d system combining the long-range Coulomb and LJ interactions. As expected, the nanoparticle growth driven by the Ostwald ripening is observed in the former case, while long-range interaction limited self-assembled nanostructures are observed in the latter case (Fig. 12).

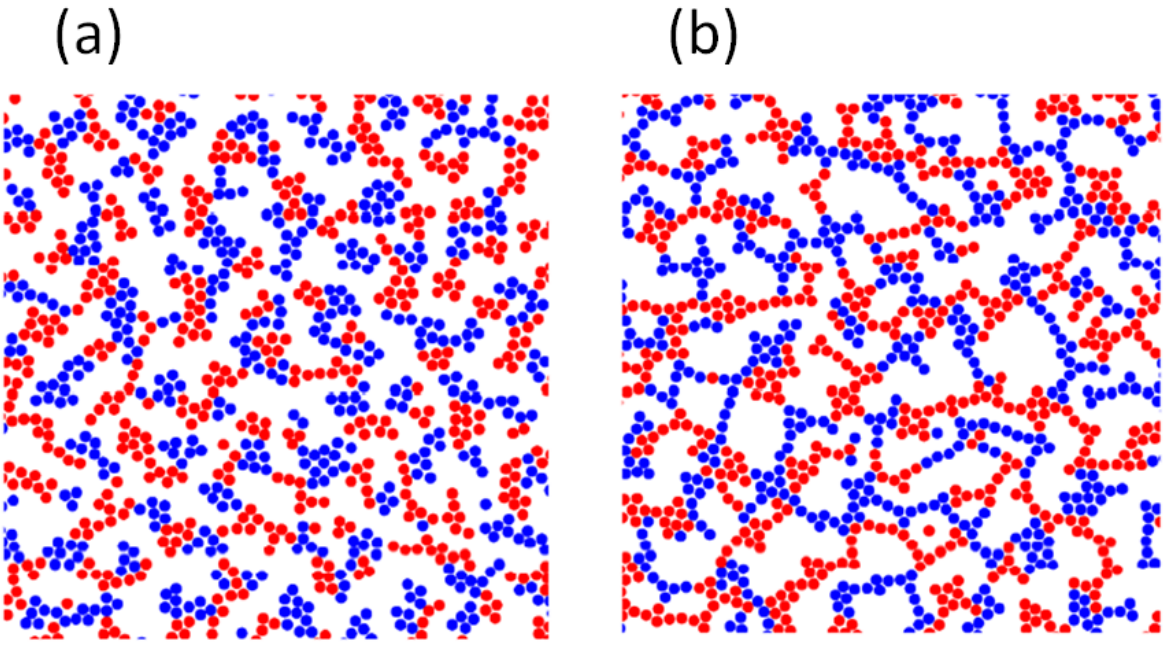

Figure 12. Aggregation in two dimensions: percolated dendritic (fractal-like) growth. Characteristic structure snapshots (small fragments) obtained using the RMC by increasing of time, (a,b).

INTERACTION OF ELECTROMAGNETIC RADIATION WITH MATTER: TIME RESOLVED APPROACH

E. Klotins

Determining the properties of electric charges excited at interaction of electromagnetic radiation is of major interest across many branches of solid state physics and advanced materials. Computational approaches to the luminescence, energy harvesting and electroconductivity rely on representing the advanced materials in terms of interacting electric charges obeying requirements of quantum mechanics, quantum field theory and relativity. Currently, there are no general efficient methods to deal with challenging problems that involves both kinetics of electrons, electron holes and their interaction with atoms constituting the material. The research is addressed to intrinsic charge transfer in dielectric materials sensitive to electromagnetic radiation within the range of visible and ultraviolet light. A special attention is paid to the time dependence of radiation field which, unlike the existing models, is arbitrary. Determining these properties relies on well-known theoretical approaches to the free particles. With application to solids distinguished by the environment of surrounding atoms these appraches become more complex and not completely understood.

What is new in the presented research is the extension of the model of noninteracting electrons and electronic holes to the back reaction of surronding atoms. This back reaction is supported by supplementary kind of particles – phonons as a challenge. In the present study, we propose a step towards this unsolved problem and derive a closed set of equations for the self-consistent treatment of electrons, the electronic holes and the back-reaction of phonons.

The key development of this work is disconnection of the electron – phonon and the electron hole – phonon interaction into purely electronic and hole parts added to the impact of electromagnetic radiation by the extra terms. Formally these extra terms contribute on equal grounds with the electromagnetic radiation with the mathematical structure of the solution maintained. Also maintained are arbitrary time dependence of radiation and full time history of the material. The necessary theory inputs are available within conventional quantum mechanics and commercial codes while the key output is the distribution function for electron – electronic hole pair determining all observables of interest.

C. Plasma Physics

DEPENDENCE OF THE GIROTRON EFFICIENCY ON ASIMUTAL INDEX OF THE NON-SYMMETRIC MODES

O. Dumbrajs,

G.S. Nusinovich, T.M. Antonsen, Jr

Institute for Research in Electronics and Applied Physics, University of Maryland, College Park, USA

Development of MW-class gyrotrons for future controlled fusion reactors requires careful analysis of the stability of high efficiency operation in very high-order modes. In the present

paper, this problem is analyzed in the framework of the non-stationary self-consistent theory of gyrotrons.

Two approaches are used: the one based on the wave envelope representation of the resonator field and the second one based on representation of this field as a superposition of eigenmodes, whose fields are determined by a self-consistent set of equations. It is shown that at relatively low beam currents, when the maximum efficiency can be realized in the regime of soft self-excitation, the operation in the desired mode is stable even in the case of a very dense spectrum of competing modes.

At higher currents, the maximum efficiency can be realized in the regimes with hard self-excitation; here the operation in the desired mode can be unstable because of the presence of some competing modes with low start currents. Two 170 GHz European gyrotrons for the international thermonuclear experimental reactor ITER are considered as examples. In the first one, which is the 2 MW gyrotron with a coaxial resonator, the stability of operation in a chosen $TE_{34,19}$-mode in the presence of two sideband modes with almost equidistant spectrum is analyzed and the region of magnetic fields in which the oscillations of the central mode are stable is determined.

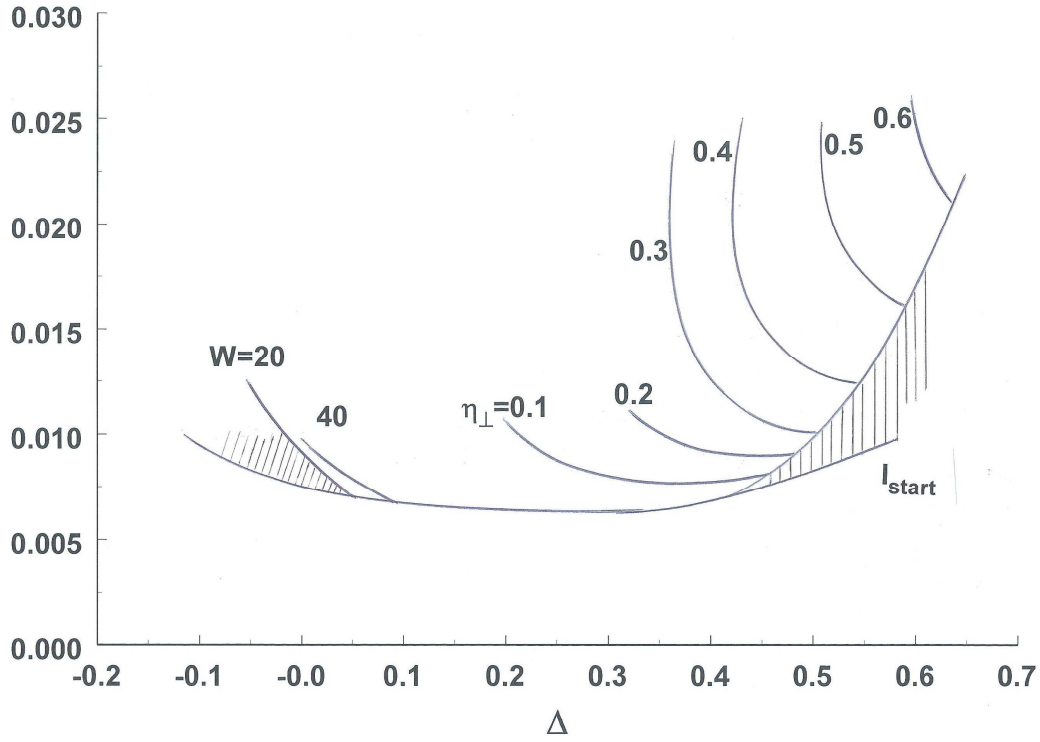

Figure 13. Region of stable operation surrounded by dashed regions in which oscillations of the operating mode are unstable. Normalized length $\varsigma_{out} = \left(\beta_{\perp 0}^2 / 2\beta_{z0}\right)\left(\omega_0 L / c\right)$ is equal to 10. Also contours of equal values of the orbital efficiency $\eta_\perp$ are shown in the region of stable operation.

The operation of the second, 1 MW gyrotron with a cylindrical cavity currently under development in Europe, is studied by using the wave envelope approach. It is shown that high efficiency operation of this gyrotron in the TE32,9-mode should be stable (Fig. 13).

ON THE DEPENDENCE OF THE EFFICIENCY 240 GHz HIGH-POWER GYROTRON ON THE DISPLACEMENT OF THE ELECTRON BEAM AND THE AZIMUTAL INDEX

O. Dumbrajs,

K.A. Avramidis, J. Franck, J. Jelonnek

Karlsruhe Institute of Technology (KIT), Institute for Pulsed Power and Microwave Technology (IHM), Association EURATOM-KIT, Karlsruhe, Germany.

Two issues in the cavity design for a Megawatt-class, 240 GHz gyrotron are addressed. Those are, firstly, the effect of a misaligned electron beam on the gyrotron efficiency and, secondly, a possible azimuthal instability of the gyrotron. The aforementioned effects are important for any gyrotron operation, but could be more critical in the operation of Megawatt-class gyrotrons at the frequencies above 200 GHz, which will be the anticipated requirement of DEMO. The target is to provide some basic trends to be considered during the refinement and optimization of the design. Self-consistent calculations are the base for simulations wherever possible. However, in cases for which self-consistent models were not available, fixed-field results are presented (Fig. 14). In those cases the conservative nature of the results should be kept in mind.

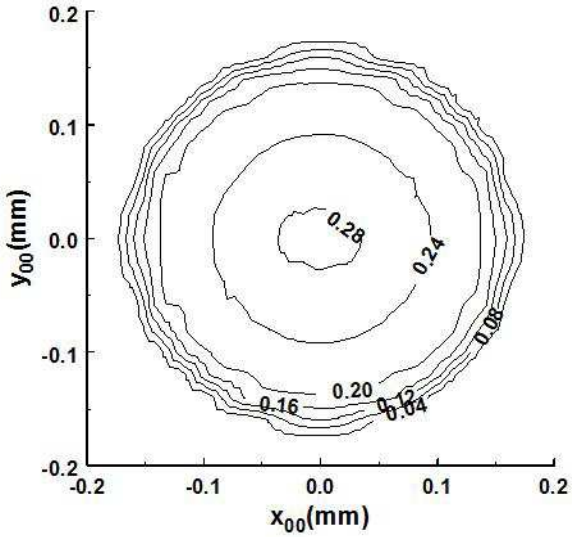

Figure 14. Fixed-field results for a parallel displacement of the electron beam (i.e. shift only, no tilt): The interaction efficiency η_{tot} is plotted as a function of the transverse coordinates. An ideal electron beam with a radius of 10 mm is assumed.

FREQUENCY TUNABILITY OF GYRO-BWO

O. Dumbrajs

G.S. Nusinovich

Institute for Research in Electronics and Applied Physics, University of Maryland, College Park, USA

Gyrotron backward-wave oscillators (gyro-BWOs) are oscillators capable of producing frequency tunable, high-power radiation at millimeter and submillimeter wavelengths (Fig. 15). While in the most advanced version of gyro-devices, the gyromonotron (or simply, the gyrotron) the variation of the external magnetic field can yield a step-tunable radiation due to the gyrotron hopping from one mode to another, in gyro-BWOs the radiation frequency can be tuned continuously. In this presentation, we discuss various concepts of gyro-BWOs offering large bandwidth and give an overview of experimental results. Some new results of simulations for frequency tunable gyro-BWOs are also presented. Part of these results is obtained in the framework of the general theory of gyro-BWO, while another part is focused on the analysis of possible frequency tunability of two gyrotrons, which are currently under development at the FIR Center of the Fukui University, Japan.

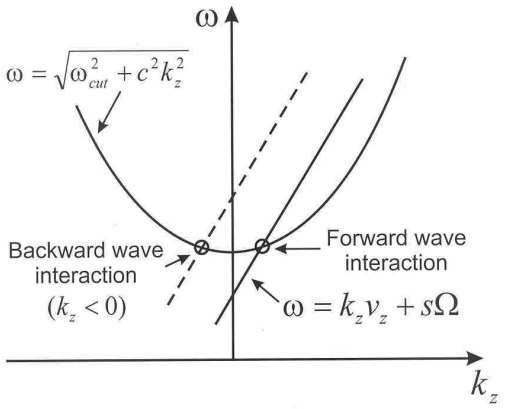

Figure 15. Dispersion diagram.

D. Experimental studies

STRUCTURE AND LUMINESCENT PROPERTIES OF $BaZrO_3$ NANOCRYSTALS IN THE POLYMER MATRIX

A.I. Popov,

O.I. Aksimentyeva, V. Savchyn,

Departments of Chemistry and Electronics, Ivan Franko National University of Lviv, Ukraine,

The effect of polymer environment on luminescent properties of barium zirconate nanocrystals have been studied by means of cathodoluminescence (CL) spectroscopy

technique (Fig. 16). It was found that polystyrene (PS) shell around $BaZrO_3$ nanocrystals significantly modify CL spectra. This phenomenon can be explained by a chemical interaction between PS and $BaZrO_3$ significantly changing the surface states of nanocrystals. This conclusion is confirmed by the complementary experimental studies including X-ray diffraction, FTIR spectroscopy, Energy Dispersive X-ray analysis and scanning electron spectroscopy.

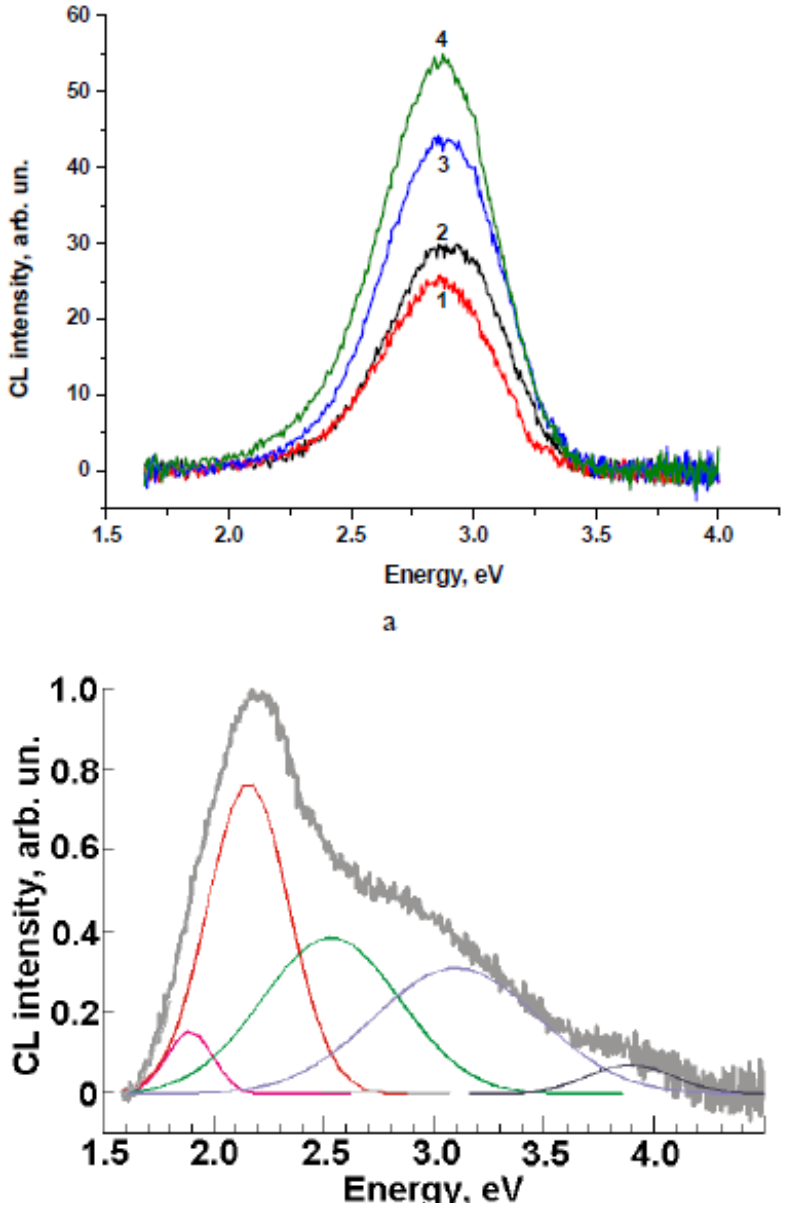

Figure 16. CL spectra of nano-$BaZrO_3$–PPA composites with a $BaZrO_3$ content of 80% (1), 90% (3) and 100% (4) and PEDOT–$BaZrO_3$ (60%) composites at T = 293 K (2); (b) CL spectrum of a PS–$BaZrO_3$ (20%) composite.

MODELING AND SYNCHROTRON DATA ANALYSIS OF MODIFIED HYDROXYAPATITE STRUCTURE

A.I. Popov

A.V. Bystrova
Institute of Theoretical and Experimental Biophysics RAS, Pushchino, Russia

Yu.D. Dekhtyar
Biomedical Engineering and Nanotechnology Institute, Riga Technical University,

V.S. Bystrov
Institute of Mathematical Problems of Biology RAS, 142290, Pushchino, Russia

The obtained results are based on the first principles modeling and calculations for hydroxyapatite (HAP) nanostructures as native as well surface modified, charged and having various defects (H and OH vacancies, H internodes). HAP structures having being studied using Local Density Approximation (LDA) method with calculations of Density of States (DOS) allow us analyzing the experimental forbidden energy gap (E_g) and work function data.

Molecular modeling by HyperChem is confirmed by photoelectron monochromatic measurements up to 6 eV and photoluminescence excitation spectra (PL) data from synchrotron DESY experimental data up to 30 eV values. Brief analysis of the influence of heating, microwave radiation, hydrogenation, x-rays and synchrotron radiation on HAP surface is presented in this work. New data of the structure of modified hydroxyapatite are obtained. The determined energy levels for H internodes is $E_{\text{H-int}} \sim Ev$ + (1.5–2.0) eV, while for OH vacancy energy is in the range of $E_{\text{OH-vac}} \sim Ev$ + (2.9–3.4) eV inside the band gap E_g.

The analysis of PL emission allows us to conclude that these energies are close to observed main PL spectral line 420 nm (2.95 eV), and consequently OH vacancy could play the leading role in the surface energy levels changes and charging. But the influence of the inserted hydrogen is revealed too through excitation from most deep valence band levels due to existence of close overlapped molecular orbital with phosphorus atoms in the excited states. Both defects are observed by PL emission spectrum under synchrotron excitation energy in diapason ~8.5–14.5 eV.

Publications in year 2014

SCI

1. T.S. Bjørheim and **E.A. Kotomin**, *Ab initio* thermodynamics of oxygen vacancies and zinc interstitials in ZnO. - J. Phys. Chem. Lett. 2014, **5**, p. 4238−4242.
2. **D. Gryaznov**, S. Baumann, **E.A. Kotomin,** and R. Merkle, Comparison of permeation measurements and hybrid density-functional calculations on oxygen vacancy transport in complex perovskite oxides. - J. Phys. Chem. C 2014, **118**, p. 29542−29553.
3. **V.N. Kuzovkov** and **E.A. Kotomin,** Static and dynamic screening effects in the electrostatic self-assembly of nano-particles. - Phys. Chem. Chem. Phys. 2014, **16**, p. 25449-25460.
4. **V.N. Kuzovkov**, **G. Zvejnieks**, and **E.A. Kotomin**, Theory of non-equilibrium critical phenomena in three-dimensional condensed systems of charged mobile nanoparticles. - Phys. Chem. Chem. Phys. 2014, **16**, p. 13974-13983.
5. E. Li, V. Igochine, **O. Dumbrajs**, L. Xu, K. Chen, T. Shi, and L. Hu, The non-resonant kink modes triggering strong sawtooth-like crashes in the EAST tokamak. - Plasma Phys. Control. Fusion 2014, **56**, 125016 (p. 1-12).
6. **O. Dumbrajs**, K.A. Avramidis, J. Franck, and J. Jelonnek, On the dependence of the efficiency of a 240 GHz high-power gyrotron on the displacement of the electron beam and on the azimuthal index. - Phys. Plasmas 2014, **21**, 013104 (p. 1-6).
7. **O. Dumbrajs**, G.S. Nusinovich, and T.M. Antonsen Jr., Dependence of the gyrotron efficiency on the azimuthal index of non-symmetric modes. - Phys. Plasmas 2014, **21**, 063112 (p. 1-8).
8. **G. Zvejnieks**, A. Ibenskas, and E.E. Tornau, Kinetic Monte Carlo modeling of reaction-induced phase separation in Au/Ni(111) surface alloy. - Surf. Coat. Technol. 2014, **255**, p. 15-21.
9. **D. Gryaznov**, M.W. Finnis, R.A. Evarestov, and J. Maier, Oxygen vacancy formation energies in Sr-doped complex perovskites: ab initio thermodynamic study. - Solid State Ionics 2014, **254**, p. 11–16.
10. H. Shi, R. Jia, and **R.I. Eglitis**, First-principles simulations of *H* centers in CaF_2. - Comp. Mater. Sci. 2014, **89**, p. 247–256.
11. A.B. Usseinov, **E.A. Kotomin**, A.T. Akilbekov, **Yu.F. Zhukovskii**, and J. Purans, Hydrogen induced metallization of ZnO($1\bar{1}00$) surface: *Ab initio* study. - Thin Solid Films 2014, **553**, p. 38–42.
12. **G. Zvejnieks**, **V.N. Kuzovkov**, and **E.A. Kotomin**, Statistical characterization of self-assembled charged nanoparticle structures. - Phys. Status Solidi A 2014, **211**, p. 288–293.
13. A. Anspoks, **D. Bocharov**, J. Purans, F. Rocca, A. Sarakovskis, V.A. Trepakov, A. Dejneka, and M. Itoh, Local structure studies of $SrTi^{16}O_3$ and $SrTi^{18}O_3$. - Phys. Scr. 2014, **89**, 044002 (p. 1-5).
14. A.B. Usseinov, **E.A. Kotomin**, A.T. Akilbekov, **Yu.F. Zhukovskii**, and J. Purans, Hydrogen adsorption on the ZnO($1\bar{1}00$) surface: ab initio hybrid density functional linear combination of atomic orbitals calculations. - Phys. Scr. 2014, **89**, 045801 (p. 1-7).

15. M.M. Kuklja, **E.A. Kotomin**, O. Sharia, **Yu.A. Mastrikov**, and J. Maier, Radiation defects in complex perovskite solid solutions. - Nucl. Instrum. Meth. B 2014, **326**, p. 243–246.
16. F.U. Abuova, **E.A. Kotomin**, V.M. Lisitsyn, A.T. Akilbekov, and **S. Piskunov**, *Ab initio* modeling of radiation damage in MgF_2 crystals. - Nucl. Instrum. Meth. B 2014, **326**, p. 314–317.
17. E.M. Khutoryan, **O. Dumbrajs**, and G.S. Nusinovich, Theoretical study of the effect of electron beam misalignment on operation of the gyrotron FU IV A. - IEEE Trans. Plasma Sci. 2014, **42**, p. 1586-1593.
18. O.I. Aksimentyeva, V.P. Savchyn, V.P. Dyakonov, S. Piechota, Yu.Yu. Horbenko, I.Ye. Opainych, P.Yu. Demchenko, **A.I. Popov**, and H. Szymczak, Modification of polymer-magnetic nanoparticles by luminescent and conducting substances. - Mol. Cryst. Liq. Cryst. 2014, **590**, p. 35–42.
19. **E. Klotins**, Phonon-assisted kinetics of electron-hole pair on two-band model. - Lith. J. Phys. 2014, **54**, p. 217–226.
20. **R.I. Eglitis**, *Ab initio* calculations of $SrTiO_3$, $BaTiO_3$, PbTiO3, $CaTiO_3$, $SrZrO_3$, $PbZrO_3$ and $BaZrO_3$ (001), (011) and (111) surfaces as well as *F* centers, polarons, KTN solid solutions and Nb impurities therein (Rev.). - Int. J. Mod. Phys. B 2014, **28**, 1430009 (p. 1-43).
21. A.V. Bystrova, Yu.D. Dekhtyar, **A.I. Popov**, and V.S. Bystrov, Modeling and Synchrotron Data Analysis of Modified Hydroxyapatite Structure. – Mathemat. Biology Bioinform. 2014, **9**, p. 171–182.

Chapters in Scientific Books

1. **Yu.F. Zhukovskii**, Boron and Metal Diborides. – Chapter 4 in book: R.A. Evarestov, Theoretical Modeling of Inorganic Nanostructures (Springer-Verlag, Berlin, Heidelberg) 2014, p. 217-251.
2. **Yu.F. Zhukovskii**, Group IV Semiconductors. – Chapter 5 in book: R.A. Evarestov, Theoretical Modeling of Inorganic Nanostructures (Springer-Verlag, Berlin, Heidelberg) 2014, p. 253-346.
3. **Yu.F. Zhukovskii**, Nitrides of Boron and Group III Metals. – Chapter 6 in book: R.A. Evarestov, Theoretical Modeling of Inorganic Nanostructures (Springer-Verlag, Berlin, Heidelberg) 2014, p. 347-427.

Non-SCI papers

1. **Yu.N. Shunin**, S. Bellucci, **Yu.F. Zhukovskii**, V.I. Gopejenko, N. Burlutskaya, T. Lobanova-Shunina, A. Capobianchi, and F. Micciulla, CNT-Fe-Pt interconnect electromagnetic simulations for magnetically stimulated CNT growth and novel memory nanodevices. – Comput. Model. New Technol. (Latvia) 2014, **18**, p. 7-23.
2. **O. Dumbrajs**, Vai magnētiskais monopols atklāts (latv.)? - Enerģija un pasaule 2014, **4**, p. 58-61.

Presentations at Scientific Conferences, Meetings, Schools and Workshops in year 2014

I. 30th ISSP Conference (Riga, Latvia, February, 2014).

1. D. Bocharov, S. Piskunov, P. Zhgun, J. Purans, and A. Kuzmin, "Lattice dynamics of cubic ScF_3 from first principles calculations". Abstract: p. 32.

2. A. Platonenko, S. Piskunov, Yu.F. Zhukovskii, and D. Bocharov, "Fe-Pt nanoparticle structure: Ab initio calculations". Abstract: p. 33.

3. J. Begens, S. Piskunov, Yu.F. Zhukovskii, and O. Lisovski, "Simulations and comparison of doped $SrTiO_3$ and TiO_2 nanotubes for application in photocatalytic water separation". Abstract: p. 35.

4. A. Gopejenko, Yu.F. Zhukovskii, P.V. Vladimirov, E.A. Kotomin, Yu.A. Mastrikov, V.A. Borodin, and A. Möslang, "First principles calculations of the energy barriers for different trajectories of Y atom migration inside fcc-Fe lattice". Abstract: p. 36.

II. 16th Israel Materials Engineering Conference (Haifa, Israel, February, 2014).

5. E.A. Kotomin, D. Fuks, M. Kuklja, Yu.A. Mastrikov, R. Merkle and J. Maier, "Ab initio modelling of pervoskite solid solutions for solid oxide fuel cells and permeation membranes". Abstract: p. 26.

III. The 5th International Workshop on Far-Infrared Technologies 2014 (Fukui, Japan, March, 2014).

6. O. Dumbrajs and G.S. Nusinovich, "Frequency tunability of the gyro-BWO". Abstract: p. 5p-6.

IV. 48th Russian School on Condensed State Physics (St. Petersburg, Russia, March, 2014).

7. D. Bocharov, S. Piskunov, O. Lisovski, J. Kazerovskis, J. Begens, Yu.F. Zhukovkii, and E. Spohr, "Quantum chemical simulations of TiO_2 nanotubes for photocatalytical water splitting". Abstract: p. 166

V. Workshop on Permeation membranes (GREEN-OTM EC Project meeting) (Valencia, Spain, March-April, 2014).

8. E.A. Kotomin and D. Gryaznov, "Ab initio modelling of a role of Sr doping in permeation membranes".

VI. Materials Research Society, MRS Spring Meeting 2014 (San Francisco, USA, April, 2014).

9. Yu.A. Mastrikov, M.M. Kuklja, R. Merkle, E.A. Kotomin, and J. Maier, "Oxygen Mobility in LSCF and BSCF Perovskites from ab Initio Modeling". Abstract: L8.02.

VII. WG4 COST Meeting, Action CM 1104 "Reducible Oxide Chemistry" (Riga, Latvia, April, 2014).

10. D. Gryaznov, J. Begens, and E.A. Kotomin, "First principles calculations on oxygen vacancy behaviour in Sr-doped complex perovskites for permeation membranes and solid oxide fuel cells". Abstract: p. 23.

11. Yu.A. Mastrikov and E.A. Kotomin, "First-principles modelling of oxygen transport in complex perovskites". Abstract: p. 29.

12. A.I. Popov, A.Ch. Lushchik, Ch.B. Lushchik, and E.A. Kotomin, "Analysis of excitonic mechanism of defect formation in insulating materials: Generalization of Rabin-Klick diagram for a whole family of alkali halides". Abstract: p. 30.

VIII. 12th International Conference "Information Technologies and Management", IT&M'2014 (Riga, Latvia, April, 2014).

13. Yu.N. Shunin, Yu.F. Zhukovskii, V.I. Gopeyenko, N. Burlutskaya, T. Lobanova-Shunina, and S. Bellucci, "Simulation of fundamental properties in CNT- and graphene-based nanoporous materials: Electromechanics and Electromagnetics". Abstract: p. 17-18.

14. Yu.F. Zhukovskii, S. Piskunov, A. Platonenko, and E.A. Kotomin, "Simulation of radiation-induced Frenkel pairs in α-Al_2O_3: Optimization of computational procedure". Abstract: p. 19-20.

15. A. Gopejenko, Yu.F. Zhukovskii, P.V. Vladimirov, Yu.A. Mastrikov, E.A. Kotomin, V.A. Borodin, and A. Möslang, "Ab initio calculations of interactions between Y, O impurity atoms and Fe vacancies for ODS steel implementation in fusion reactors". Abstract: p. 21-22.

16. A. Platonenko, S. Piskunov, D. Bocharov, Yu.F. Zhukovskii, and S. Bellucci, "First principles simulations on Fe-Pt nanoclusters of various morphology and CNT growth upon them". Abstract: p. 23-25.

17. A. Chesnokov, O. Lisovski, D. Bocharov, S. Piskunov, Yu.F. Zhukovskii, M. Wessel, and E. Spohr, "Quantum-chemical study of pristine and doped TiO_2 nanotubes for water photocatalysis". Abstract: p. 26-28.

18. P. Zhgun, D. Bocharov, S. Piskunov, J. Purans, and A. Kuzmin, "Ab initio calculations on electronic structure and phonons in cubic ScF_3". Abstract: p. 169-170.

IX. E-MRS 2014 Spring Meeting (Lille, France, May, 2013).

19. R.I. Eglitis, „Towards a practical rechargeable 5 V Li ion battery". – Abstract: BB.1.2.

20. E.A. Kotomin, M.M. Kuklja, D. Fuks, Yu.A. Mastrikov, and J. Maier, „A comparative study of structural stability of complex perovskites for solid oxide fuel cells: First principles thermodynamic calculations". – Abstract: C.4.4.

21. R.I. Eglitis, „Ab initio calculations of $SrTiO_3$, $BaTiO_3$, $PbTiO_3$ and $CaTiO_3$ (001), (011) and (111) surfaces". – Abstract: C.4.7.

22. A.U. Abuova, T.M. Inerbaev, A.T. Akilbekov, Yu.A. Mastrikov, and E.A. Kotomin, „First principles modeling of Ag adsorption on the MnO_2- and LaO-terminated surfaces of $LaMnO_3$(001)". – Abstract: C/P1.1.

23. G. Kaptagai, T.M. Inerbaev, A.T. Akilbekov, Yu.A. Mastrikov, and E.A. Kotomin, „Water interaction with fluorine-doped Co_3O_4 (100) and (111) surfaces". – Abstract: C/P1.10.

24. Yu.A. Mastrikov, E.A. Kotomin, R. Merkle, M.M. Kuklja, and J. Maier, „First principles calculations of formation and migration of oxygen vacancies in the bulk and at the surface of complex perovskites for solid oxide fuel cell cathodes". – Abstract: C/P1.11.

25. E.A. Kotomin, R. Merkle, Yu.A. Mastrikov, M.M. Kuklja, and J. Maier, „Ab initio modeling of oxygen reduction reaction in mixed conducting perovsites for solid oxide fuel cells". – Abstract: CC.1.6.

26. M. Arrigoni, D. Gryaznov, E.A. Kotomin, and J. Maier, „Confinement effects for ionic carriers in ABO_3 perovskite ultrathin films". – Abstract: EO.5.3.

27. Yu.F. Zhukovskii, S. Piskunov, O. Lisovskii, J. Begens, and E. Spohr, „Doped TiO_2 and $SrTiO_3$ nanotubes for photocatalytic applications: Predictions from first principles". – Abstract: EO.8.2.

28. R.I. Eglitis, H. Shi, and R. Jia, „Ab initio calculations of the transfer and aggregation of F centers, as well as bulk and nano-surface H centers in CaF_2, BaF_2 and SrF_2". – Abstract: EP.1.9.

29. A.I. Popov, L. Shirmane, V. Pankratov, A.Ch. Lushchik, V.E. Serga, A. Kotlov, and J. Zimmermann, „Luminescence of macro- and nanocrystalline MgO excited by VUV synchrotron radiation". – Abstract: EP.2.54.

30. Yu.A. Mastrikov, P.V. Vladimirov, V.A. Borodin, A. Gopejenko, Yu.F. Zhukovskii, E.A. Kotomin, and A. Möslang, „Ab initio simulation of the initial steps of the ODS particle formation process in bcc iron matrix". – Abstract: EP.2.73.

31. I. Karbovnyk, P. Savchyn, A. Huczko, M. Cestelli-Guidi, C Mirri, and A.I. Popov, „FTIR studies of silicon carbide nanostructures". – Abstract: G.PII.37.

32. A.I. Popov, V. Savchyn, J. Purans, A. Dabrowska, A. Huczko, B. Pathak, and D.P. Subedi, „Cathodoluminescence study of Al-doped ZnO nanofilms at 80 K and RT". – Abstract: I.P3.43.

33. O. Aksimentyeva, V. Savchyn, I. Opaynych, P. Demchenko, Yu. Horbenko, V. Pankratov, and A.I. Popov, „Effect of polymer matrix on the structure and luminescence properties of barium zirconate ($BaZrO_3$) nanocrystals". – Abstract: Q.P1.62.

34. R.I. Eglitis, H. Shi, and R. Jia, „Ab initio calculations of the self trapped hole in SrF_2, as well as bulk and surface hydroxyl impurities in CaF_2 and BaF_2". – Abstract: U.1.2.

X. International Symposium on Reactivity of Solids, (St. Petersburg, Russia, June, 2014).

35. E.A. Kotomin, R. Merkle, Yu.A. Mastrikov, M.M. Kuklja, and J. Maier, "Ab initio modelling of oxygen reduction reaction in mixed conducting pervoskites for solid oxide fuell cells". Abstract: p. 99.

XI. DSL2014 conference (Paris, France, June, 2014).

36. V.N. Kuzovkov, M. Olvera de la Cruz, G. Zvejnieks, and E.A. Kotomin, "Diffusion and self-assembly of charged nanoparticles in three-dimensional condensed systems". Abstract: p. 214.

XII. Electrochemistry workshop, (Asilomar, USA, July, 2014).

37. E.A. Kotomin, Yu. Mastrikov, and M. Kuklja, "Structural instability of perovskite solid solutions".

XIII. Proceedings 9th International Workshop Strong Microwaves and Terahertz Waves: Sources and Applications, (Nizhny Novgorod, Russia, July, 2014).

38. O. Dumbrajs, G.S. Nusinovich, and T.M. Antonsen, "Stability of gyrotron operation in very high order modes". Abstract: p. 154.

XIV. 4th International Workshop on Nanocarbon Photonics and Optoelectronics (Polvijärvi, Finland, July-August, 2014).

39. Yu.N. Shunin, Yu.F. Zhukovskii, V.I. Gopeyenko, N. Burlutskaya, T. Lobanova-Shunina, and S. Bellucci, "Simulation of electromagnetic properties in CNT- and graphene-based nanomaterials and nanodevices". Abstract: p. 74.

XV. International conference on solid state protonic conductors (SSPC-17) (Seoul, Korea, September, 2014).

40. T. Bjørheim, E.A. Kotomin, R. Haugsrud, and J. Maier, "Defect thermodynamics of $BaZrO_3$ from first principles phonon calculations".

XVI. E-MRS 2014 Fall Meeting, (Warsaw, Poland, September, 2014).

41. D. Gryaznov, "First principles calculations on oxygen vacancy behaviour in Sr-doped complex perovskites for permeation membranes and solid oxide fuel cells". Abstract: A5.21.

42. R.I. Eglitis, "Point defects and surfaces in perovskite structured oxides". Abstract: D13.1.

43. D. Gryaznov, D. Bocharov, E.A. Kotomin, and Yu.F Zhukovskii, "Ab initio simulations of oxygen interaction with surfaces and interfaces in uranium mononitride". Abstract: G9.44.

44. R.I. Eglitis, H. Shi and R. Jia, "Ab initio calculations of F, R, bulk and surface H centers, as well as hydroxyl impurities in CaF_2, BaF_2 and SrF_2". Abstract: K2.6.

45. R.I. Eglitis, "Towards a practical rechargeable 5 V Li ion battery". Abstract: S9.1.

XVII. Joint 12th RCBJCF Symposium and 9th FMNT Conference (Riga, Latvia, September-October, 2014).

46. R. Merkle, D. Poetzsch, D. Gryaznov, E.A. Kotomin, and J. Maier, "Mixed conducting perovskites as solid oxide fuel cell cathode materials: Insight from experiments and theory". Abstract: p. 75.

47. E. Spohr, M. Wessel, D. Bocharov, and S. Piskunov, "Simulation of oxide nanostructures for energy conversion". Abstract: p. 99.

48. A. Anspoks, D. Bocharov, J. Purans, F. Rocca, A. Sharakovskis, J. Timoshenko, V.A. Trepakov, A. Dejneka, and M. Itoh, "Local structure studies of Ti for $SrTi^{16}O_3$ and $SrTi^{18}O_3$ by advanced X-ray absorption spectroscopy data analysis. Abstract: p. 124.

49. Yu.F. Zhukovskii, R.A. Evarestov, and A.V. Bandura, "First principles simulations on stoichiometric $SrTiO_3$ nanowires'. Abstract: p. 160.

50. R.I. Eglitis, H. Shi, and R. Jia, "First principles calculations of the diffusion and aggregation of F centers as well as bulk and nano-surface H centers in CaF_2, BaF_2 and SrF_2". Abstract: p. 166.

51. R.I. Eglitis, "First principles calculations of $SrTiO_3$, $BaTiO_3$, $PbTiO_3$ and $CaTiO_3$ (001), (011) and (111) surfaces". Abstract: p. 167.

52. I. Bolesta, I. Karbovnyk, I. Rovetsky, S. Velgosh, I. Kityk, and A.I. Popov, "Effects of long term annealing on the nanostructures formed in CdI_2 crystals". Abstract: p. 180.

53. V.P. Savchyn, O.I. Aksimentyeva, Yu.Yu. Horbenko, I. Karbovnyk, V. Pankratov, and A.I. Popov, "Cathodoluminescence characterization of polystyrene–$BaZrO_3$ hybrid composites". Abstract: p. 181.

54. T.S. Bjørheim, R. Haugsrud, J. Maier, and E.A. Kotomin, "Defect thermodynamics of $BaZrO_3$ from first principles phonon calculations". Abstract: p. 237.

55. R.I. Eglitis, "Towards a practical rechargeable 5 V Li ion battery". Abstract: p. 242.

56. E.A. Kotomin, M.M. Kuklja, Yu.A. Mastrikov, R. Merkle, and J. Maier, "Challenges in energy applications of non-stoichiometric complex perovskites". Abstract: p. 247.

57. Yu.N. Shunin, Yu.F. Zhukovskii, V.I. Gopeyenko, N. Burlutskaya, T. Lobanova-Shunina, and S. Bellucci, "Electromechanics and electromagnetics of CNT- and graphene-based nanoporous materials: Interconnects and nanosensoring". Abstracts: p. 264.

58. A.U. Abuova, T.M. Inerbaev, E.A. Kotomin, A.T. Akilbekov, and Yu.A. Mastrikov, "Ab Initio modelling of Ag adsorption on the MnO_2- and LaO-terminated LMO(001) surfaces". Abstracts: p. 271.

59. A. Chesnokov, O. Lisovskii, D. Bocharov, S. Piskunov, Yu.F. Zhukovskii, M. Wessel, and E. Spohr, "Ab initio simulations on N and S co-doped titania nanotubes for photocatalytic applications". Abstracts: p. 272.

60. A. Usseinov, E.A. Kotomin, Yu.F. Zhukovskii, J. Purans, A.T. Akilbekov, and A.K. Dauletbekova, "Electronic effects on hydrogen-adsorbed surfaces of ZnO: First principles study". Abstracts: p. 275.

61. A. Platonenko, S. Piskunov, Yu.F. Zhukovskii, and E.A. Kotomin, "Ab initio simulations on Frenkel pairs of radiation defects in corundum". Abstracts: p. 278.

62. E. Klotins, "Relativistic time-resolved approach for phonon-assisted interaction between electron and intensive radiation field". Abstracts: p. 281.

63. A. Gopejenko, Yu.F. Zhukovskii, P.V. Vladimirov, E.A. Kotomin, Yu.A. Mastrikov, V.A. Borodin, and A. Möslang, "Ab initio calculations of interactions between Y and O impurity atoms and vacancies in bcc- and fcc-iron lattices". Abstracts: p. 282.

64. D. Bocharov, S. Piskunov, P. Zhgun, J. Purans, and A. Kuzmin, "R and M mode softness in cubic ScF_3: Predictions from first principles". Abstracts: p. 283.

65. V. Savchyn, C. Balasubramanian, A. Moskina, I. Karbovnyk, and A.I. Popov, "Cathodoluminescence studies of nanostructured AlN and AlN/CsI". Abstracts: p. 313.

66. A.I. Popov, A.Ch. Lushchik, Ch.B. Lushchik, and E.A. Kotomin, "Analysis of excitonic mechanism of defect formation in insulating materials: Generalization of Rabin-Klick diagram for a whole family of alkali halides". Abstracts: p. 333.

67. G. Kaptagay, T.M. Inerbaev, E.A. Kotomin, A.T. Akilbekov, Yu.A. Mastrikov, and F.U. Abuova, "Research of interaction fluorine-doped Co_3O_4 (100) and (111) surfaces with water". Abstracts: p. 340.

XVIII. 15th International Workshop on Nanoscience and Nanotechnology, n&n-2014 (Frascati, Italy, October, 2014).

68. Yu.N. Shunin, S. Bellucci, Yu.F. Zhukovskii, V.I. Gopeyenko, T. Lobanova-Shunina, and N. Burlutskaya, "Nanocarbon-based Fe-Pt spintronic devices: models and simulation".

XIX. Materials Science and Technology (MS&T-14) (Pittsburgh, USA, October, 2014).

69. E.A. Kotomin, R. Merkle, Yu. Mastrikov, M.M. Kuklja, and J. Maier, "First principles calculations of oxygen transport in SOFC cathode materials". Abstracts, p.53.

70. M.M. Kuklja, E.A. Kotomin, D. Fuks, Yu. Mastrikov, and O. Sharia, "Disorder and structural stability of complex perovskites for solid oxide fuel cells: ab initio modeling". Abstracts, p. 103.

71. E.A. Kotomin, M. Arrigoni, D. Gryaznov, T. Bjørheim, and J. Maier, "Confinement effects for ionic carriers in $BaZrO_3$ ultrathin films". Abstracts, p. 148.

XXI. Atomistic Simulations of Functional Materials (Moscow, Russia, December, 2014).

72. E.A. Kotomin, "Computer modeling of new materials from first principles".